

# Spin observables for pion photoproduction on the deuteron in the $\Delta(1232)$ -resonance region

Eed M. Darwish <sup>†</sup>

Physics Department, Faculty of Science, South Valley University, Sohag 82524, Egypt

**Abstract.** Spin observables for the three charge states of the pion for the pion photoproduction reaction on the deuteron,  $\gamma d \rightarrow \pi NN$ , with polarized photon beam and/or oriented deuteron target are predicted. For the beam-target double-spin asymmetries, it is found that only the longitudinal asymmetries  $T_{20}^\ell$  and  $T_{2\pm 2}^\ell$  do not vanish, whereas all the circular and the other longitudinal asymmetries do vanish. The sensitivity of spin observables to the model deuteron wave function is investigated. It has been found that only  $T_{21}$  and  $T_{22}$  are sensitive to the model deuteron wave function, in particular in the case of  $\pi^0$ -production above the  $\Delta$ -region, and that other asymmetries are not.

PACS numbers: 24.70.+s, 14.20.-c, 13.60.Le, 25.20.Lj, 21.45.+v

Submitted to: *J. Phys. G: Nucl. Part. Phys.*

## 1. Introduction

Single-pion photoproduction has been a subject of extensive theoretical and experimental investigation for many decades (for an overview see, e.g., [1, 2, 3]). This reaction is one of the main sources of information on nucleon structure. It allows investigation of resonance excitations of the nucleon, especially the  $\Delta(1232)$ -excitation, and their photodecay amplitudes. The pion photoproduction amplitude on the free nucleon is used as an input when calculating pion photoproduction from heavier nuclei.

Pion photoproduction on light nuclei is primarily motivated by the study of the elementary neutron amplitude in the absence of a neutron target and the investigation of medium effects. It provides an interesting means to study nuclear structure and gives information on pion production on off-shell nucleon, as well as on the very important  $\Delta N$ -interaction in a nuclear medium. The deuteron plays an outstanding role in the investigation of pseudoscalar meson production in electromagnetic reactions since its structure is very well understood in comparison to heavier nuclei. Furthermore, the small binding energy of nucleons in the deuteron allows one to compare the contributions of its

<sup>†</sup> *E-mail address:* eeddarwish@yahoo.com

constituents to the electromagnetic and hadronic reactions to those from free nucleons in order to estimate interaction effects.

During the last decade, several experiments have been performed, e.g., at MAMI in Mainz, ELSA in Bonn, LEGS in Brookhaven, and JLab in Newport News, for preparing polarized beams and targets and for polarimeters for the polarization analysis of ejected particles (see [2, 3, 4] and references therein). Therefore, it appears timely to study in detail polarization observables in pion production on the deuteron. The aim will be to see what kind of information is buried in the various polarization observables, in particular, what can be learned about the role of subnuclear degrees of freedom like meson and isobar or even quark-gluon degrees of freedom.

Polarization observables for  $\pi^-$ -photoproduction on the deuteron via the reaction  $d(\gamma, \pi^-)pp$  have been studied within a diagrammatic approach [5]. In that work, predictions for analyzing powers connected to beam and target polarization, and to polarization of one of the final protons are presented. In our previous evaluation [6, 7], the energy dependence of the three charge states of the pion for incoherent pion photoproduction on the deuteron in the  $\Delta(1232)$ -resonance region has been investigated. We have presented results for differential and total cross sections as well as results for the beam-target spin asymmetry which determines the Gerasimov-Drell-Hearn (GDH) sum rule. Most recently, we have predicted results for the  $\pi$ -meson spectra, single- and double-spin asymmetries for incoherent pion photoproduction on the deuteron in the  $\Delta(1232)$ -resonance region [8, 9]. In particular, we have studied in detail the interference of the nonresonant background amplitudes with the dominant  $\Delta$ -excitation amplitude. We found that interference of Born terms and the  $\Delta(1232)$ -contribution plays a significant role in the calculations. The vector target asymmetry  $T_{11}$  has been found to be very sensitive to this interference.

In this paper we study several polarization observables of photon and deuteron target for the three charge states of the pion in photoproduction of  $\pi$ -mesons on the deuteron in the  $\Delta$ -resonance region with special emphasis on double-spin asymmetries. We will also compare our predictions for the linear photon asymmetry with recent experimental data from LEGS [10]. Furthermore, we will discuss the dependence of our results for single- and double-polarization observables on the model deuteron wave function. Moreover, the complete formal expressions of polarization observables for the reaction  $\vec{\gamma}\vec{d} \rightarrow \pi NN$  will be given in this paper. The particular interest in the double-polarization asymmetries for the reaction  $\vec{d}(\vec{\gamma}, \pi)NN$  is based on the fact that, a series measurements of double-polarization asymmetries in photoreactions on the proton, neutron, and deuteron have been carried out or planned at different laboratories (see, for example, [10, 11]). To provide information for these experiments involving polarized incident photon beam and polarized deuteron target, we present in this paper various spin observables.

The paper is organized as follows. In Sec. 2, we introduce the general form of the differential cross section for the reaction  $d(\gamma, \pi)NN$  and present the treatment of the transition amplitude which based on time-ordered perturbation theory. The complete

formal expressions of polarization observables for the  $\gamma d \rightarrow \pi NN$  reaction with polarized photon beam and/or oriented deuteron target in terms of the transition matrix elements are given in Sec. 3. Details of the actual calculations and the results will be presented and discussed in Sec. 4. The conclusions are summarized in Sec. 5. Explicit expressions for double-spin observables are given in Appendix A.

## 2. Pion photoproduction on the deuteron

Since the formalism of the incoherent pion photoproduction reaction on the deuteron  $\gamma d \rightarrow \pi NN$  has been described in details in our previous work [6, 8], we will indicate here only the necessary notations and definitions.

The general expression of the five-fold differential cross section is given by [12]

$$d^5\sigma = (2\pi)^{-5}\delta^4(k + d - p_1 - p_2 - q) \frac{1}{|\vec{v}_\gamma - \vec{v}_d|} \frac{1}{2} \frac{d^3q}{2\omega_{\vec{q}}} \frac{d^3p_1}{E_1} \frac{d^3p_2}{E_2} \frac{M_N^2}{4\omega_\gamma E_d} \times \frac{1}{6} \sum_{smtm_\gamma m_d} |\mathcal{M}_{smtm_\gamma m_d}^{(t\mu)}|^2, \quad (1)$$

where the definition of all kinematical variables and quantum numbers are given in [6]. This expression is evaluated in the laboratory frame or deuteron rest frame (see Fig. 4 in [6]).

Recalling the derivation given in [6], the differential cross section of incoherent pion photoproduction on the deuteron takes the form

$$\frac{d^2\sigma}{d\Omega_\pi} = \int_0^{q_{max}} dq \int d\Omega_{p_{NN}} \frac{\rho_s}{6} \sum_{smtm_\gamma m_d} |\mathcal{M}_{smtm_\gamma m_d}^{(t\mu)}|^2, \quad (2)$$

where the maximal pion momentum  $q_{max}$  is determined by the kinematics and  $\rho_s$  is the phase space factor.

The general form of the photoproduction transition matrix is given by

$$\mathcal{M}_{smtm_\gamma m_d}^{(t\mu)}(\vec{k}, \vec{q}, \vec{p}_1, \vec{p}_2) = {}^{(-)}\langle \vec{q} \mu, \vec{p}_1 \vec{p}_2 s m t - \mu | \epsilon_\mu(m_\gamma) J^\mu(0) | \vec{d} m_d 00 \rangle, \quad (3)$$

where  $J^\mu(0)$  denotes the current operator and  $\epsilon_\mu(m_\gamma)$  the photon polarization vector. The electromagnetic interaction consists of the elementary production process on one of the nucleons  $T_{\pi\gamma}^{(j)}$  ( $j = 1, 2$ ) and in principle a possible irreducible two-body production operator  $T_{\pi\gamma}^{(NN)}$ . The final  $\pi NN$  state is then subject to the various hadronic two-body interactions as described by an half-off-shell three-body scattering amplitude  $T^{\pi NN}$ . In the following, we will neglect the electromagnetic two-body production  $T_{\pi\gamma}^{(NN)}$  and the outgoing  $\pi NN$  scattering state is approximated by the free  $\pi NN$  plane wave, i.e.,

$$|\vec{q} \mu, \vec{p}_1 \vec{p}_2 s m t - \mu\rangle^{(-)} = |\vec{q} \mu, \vec{p}_1 \vec{p}_2 s m t - \mu\rangle. \quad (4)$$

This means, we include only the pure plane wave impulse approximation (IA), which is defined by the electromagnetic pion production on one of the nucleons alone, while a more realistic treatment including final-state interaction (FSI) as well as two-body effects will be reported in a forthcoming paper.

The wave function of the final  $NN$ -state in a coupled spin-isospin basis which satisfies the symmetry rules with respect to a permutation of identical nucleons has the form

$$|\vec{p}_1, \vec{p}_2, sm, t-\mu\rangle = \frac{1}{\sqrt{2}} \left( |\vec{p}_1\rangle^{(1)} |\vec{p}_2\rangle^{(2)} - (-)^{s+t} |\vec{p}_2\rangle^{(1)} |\vec{p}_1\rangle^{(2)} \right) |sm, t-\mu\rangle, \quad (5)$$

where the superscript indicates to which particle the ket refers. The deuteron wave function has the form

$$\langle \vec{p}_1 \vec{p}_2, 1m, 00 | \vec{d} m_d, 00 \rangle = (2\pi)^3 \delta^3(\vec{d} - \vec{p}_1 - \vec{p}_2) \frac{\sqrt{2 E_1 E_2}}{M_N} \tilde{\Psi}_{m, m_d}(\vec{p}_{NN}) \quad (6)$$

with

$$\tilde{\Psi}_{m, m_d}(\vec{p}) = (2\pi)^{\frac{3}{2}} \sqrt{2 E_d} \sum_{L=0,2} \sum_{m_L} i^L C_{m_L m m_d}^{L11} u_L(p) Y_{L m_L}(\hat{p}), \quad (7)$$

denoting with  $C_{m_1 m_2 m}^{j_1 j_2 j}$  a Clebsch-Gordan coefficient,  $u_L(p)$  the radial deuteron wave function and  $Y_{L m_L}(\hat{p})$  a spherical harmonics.

The matrix elements are then given in the laboratory system by

$$\begin{aligned} \mathcal{M}_{sm m_\gamma m_d}^{(t\mu)}(\vec{k}, \vec{q}, \vec{p}_1, \vec{p}_2) = \sqrt{2} \sum_{m'} & \langle sm, t-\mu | \left( \langle \vec{p}_1 | t_{\gamma\pi}(\vec{k}, \vec{q}) | -\vec{p}_2 \rangle \tilde{\Psi}_{m', m_d}(\vec{p}_2) \right. \\ & \left. - (-)^{s+t} (\vec{p}_1 \leftrightarrow \vec{p}_2) \right) | 1m', 00 \rangle, \end{aligned} \quad (8)$$

where  $t_{\gamma\pi}$  denotes the elementary production amplitude on the free nucleon.

### 3. Definition of polarization observables

The most general expression for all possible polarization observables for incoherent pion photoproduction on the deuteron is given in terms of the transition  $\mathcal{M}$ -matrix elements by [8, 13]

$$\begin{aligned} \mathcal{O} &= Tr(\mathcal{M}^\dagger \Omega \mathcal{M} \rho) \\ &= \sum_{\substack{smt m_\gamma m_d \\ s' m' t' m'_\gamma m'_d}} \int_0^{q_{max}} dq \int d\Omega_{p_{NN}} \rho_s \mathcal{M}_{s' m', m'_\gamma m'_d}^{(t' \mu')} \star \vec{\Omega}_{s' m' sm} \\ &\quad \times \mathcal{M}_{sm, m_\gamma m_d}^{(t\mu)} \rho_{m_\gamma m'_\gamma}^\gamma \rho_{m_d m'_d}^d, \end{aligned} \quad (9)$$

where  $\rho_{m_\gamma m'_\gamma}^\gamma$  and  $\rho_{m_d m'_d}^d$  denote the density matrices of initial photon polarization and deuteron orientation, respectively.  $\vec{\Omega}_{s' m' sm}$  is an operator associated with the observable, which acts in the two-nucleon spin space.

As shown in [8, 13] all possible polarization observables for the reaction  $d(\gamma, \pi)NN$  with polarized photon beam and/or polarized deuteron target can be expressed in terms of the quantities

$$\begin{aligned} V_{IM} &= \frac{1}{2\sqrt{3}} \sum_{smt, m_\gamma m_d m'_d} (-)^{1-m'_d} \sqrt{2I+1} \begin{pmatrix} 1 & 1 & I \\ m_d & -m'_d & -M \end{pmatrix} \\ &\quad \times \int_0^{q_{max}} dq \int d\Omega_{p_{NN}} \rho_s \mathcal{M}_{sm, m_\gamma m_d}^{(t\mu)} \star \mathcal{M}_{sm, m_\gamma m'_d}^{(t\mu)}, \end{aligned} \quad (10)$$

and

$$W_{IM} = \frac{1}{2\sqrt{3}} \sum_{smt, m_\gamma m_d m'_d} (-)^{1-m'_d} \sqrt{2I+1} \begin{pmatrix} 1 & 1 & I \\ m_d & -m'_d & -M \end{pmatrix} \times \int_0^{q_{max}} dq \int d\Omega_{p_{NN}} \rho_s \mathcal{M}_{sm, m_\gamma m_d}^{(t\mu)} \star \mathcal{M}_{s-m, m_\gamma -m'_d}^{(t\mu)}, \quad (11)$$

where the Wigner  $3j$ -symbols are given by [14]

$$\begin{pmatrix} 1 & 1 & I \\ m_d & -m'_d & -M \end{pmatrix} = \frac{(-)^M}{\sqrt{2I+1}} C_{m_d - m'_d - M}^{11I}. \quad (12)$$

These quantities have the symmetry properties

$$\begin{aligned} V_{IM}^* &= (-1)^M V_{I-M}, \\ W_{IM}^* &= (-1)^I W_{IM}. \end{aligned} \quad (13)$$

The unpolarized differential cross section is then given by

$$\frac{d^2\sigma}{d\Omega_\pi} = V_{00}. \quad (14)$$

A quantity of great interest is the photon asymmetry for linearly polarized photons, which takes the form

$$\Sigma \frac{d^2\sigma}{d\Omega_\pi} = -W_{00}. \quad (15)$$

The vector target asymmetry is given by

$$T_{11} \frac{d^2\sigma}{d\Omega_\pi} = 2 \Im m V_{11}. \quad (16)$$

The tensor target asymmetries can be written as

$$T_{2M} \frac{d^2\sigma}{d\Omega_\pi} = (2 - \delta_{M0}) \Re e V_{2M}, \quad M = 0, 1, 2. \quad (17)$$

The explicit expressions for single-spin asymmetries are given in our previous work [8].

The photon and target double-polarization asymmetries are given by

(i) Circular asymmetries

$$T_{1M}^c \frac{d^2\sigma}{d\Omega_\pi} = (2 - \delta_{M0}) \Re e V_{1M}, \quad M = 0, 1, \quad (18)$$

$$T_{2M}^c \frac{d^2\sigma}{d\Omega_\pi} = 2 \Im m V_{2M}, \quad M = 0, 1, 2, \quad (19)$$

(ii) Longitudinal asymmetries

$$T_{1M}^\ell \frac{d^2\sigma}{d\Omega_\pi} = i W_{1M}, \quad M = 0, \pm 1, \quad (20)$$

$$T_{2M}^\ell \frac{d^2\sigma}{d\Omega_\pi} = -W_{2M}, \quad M = 0, \pm 1, \pm 2. \quad (21)$$

We list explicit expressions of all double-polarization asymmetries for polarized photon beam and oriented deuteron target in terms of the transition matrix elements in Appendix A.

#### 4. Results and discussion

In this section we present our predictions of the polarization observables defined in Sec. 3. The contribution to the pion production amplitude in (8) is evaluated by taking a realistic  $NN$  potential model for the deuteron wave function. In our calculations, the wave function of the Paris potential [15] has been used. For the elementary pion photoproduction operator, the effective Lagrangian model of Schmidt *et al.* [16] has been considered.

The discussion of our results is divided into two parts. In order to give a complete overview on all possible polarization observables for the reaction  $d(\gamma, \pi)NN$ , we first discuss the single-spin asymmetries  $\Sigma$ ,  $T_{11}$ ,  $T_{20}$ ,  $T_{21}$ , and  $T_{22}$  as functions of pion angle at values for photon lab-energies different from that presented in our previous work [8]. In the second part, we consider the double-polarization asymmetries for photon and deuteron target as functions of emission pion angle for all the three isospin channels of the  $\vec{d}(\vec{\gamma}, \pi)NN$  reaction at nine different values of photon lab-energy  $\omega_\gamma = 250, 290, 310, 340, 360, 390, 420, 470$ , and 500 MeV.

##### 4.1. Single-spin asymmetries

Let us start by discussing the results for single-spin asymmetries for pion photoproduction on the deuteron with polarized photon beam or polarized deuteron target as shown in Figs. 1 through 6.

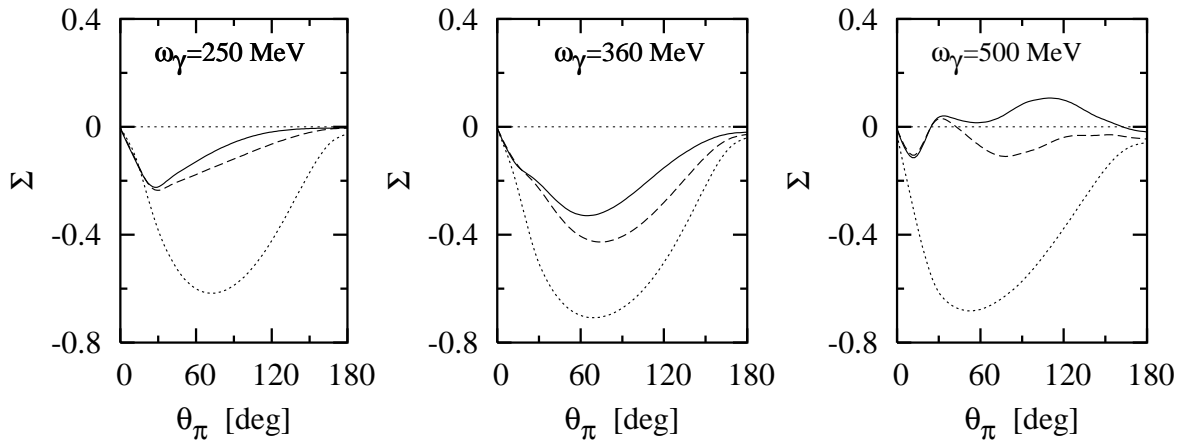


**Figure 1.** Calculated linear photon asymmetry  $\Sigma$  for the  $d(\vec{\gamma}, \pi)NN$  reaction as a function of pion angle  $\theta_\pi$  in the laboratory frame at  $\omega_\gamma = 250$  MeV (left panel), 360 MeV (middle panel), and 500 MeV (right panel) using the deuteron wave function of the Paris potential [15]. The solid, dashed, and dotted curves correspond to  $\vec{\gamma}d \rightarrow \pi^- pp$ ,  $\pi^+ nn$ , and  $\pi^0 np$ , respectively.

The photon asymmetry  $\Sigma$  for linearly polarized photons at three values of photon lab-energy  $\omega_\gamma = 250, 360$ , and 500 MeV is plotted in Fig. 1 as a function of pion angle

$\theta_\pi$  in the laboratory frame using the deuteron wave function of the Paris potential [15]. The solid, dashed, and dotted curves show the results for the  $\vec{\gamma}d \rightarrow \pi^- pp$ ,  $\pi^+ nn$ , and  $\pi^0 np$  channels, respectively. In general, we see that the linear photon asymmetry has negative values at forward and backward emission pion angles for charged and neutral pion channels. Only at  $\omega_\gamma = 500$  MeV, positive values are found for  $\pi^-$  production channel when  $\theta_\pi$  changes from  $90^\circ$  to  $150^\circ$ . One notes qualitatively a similar behaviour for charged pion channels whereas a different behaviour is seen for the neutral pion channel.

At extreme forward pion angles (below  $\theta_\pi = 10^\circ$ ), one sees that  $\Sigma$  has approximately the same values for charged as well as for neutral pion production channels, whereas a big difference between both channels is seen when  $\theta_\pi$  changes from  $30^\circ$  to  $150^\circ$ . It is also noticeable, that the asymmetry  $\Sigma$  is vanished at  $\theta_\pi = 0^\circ$  which is not the case at  $180^\circ$ .

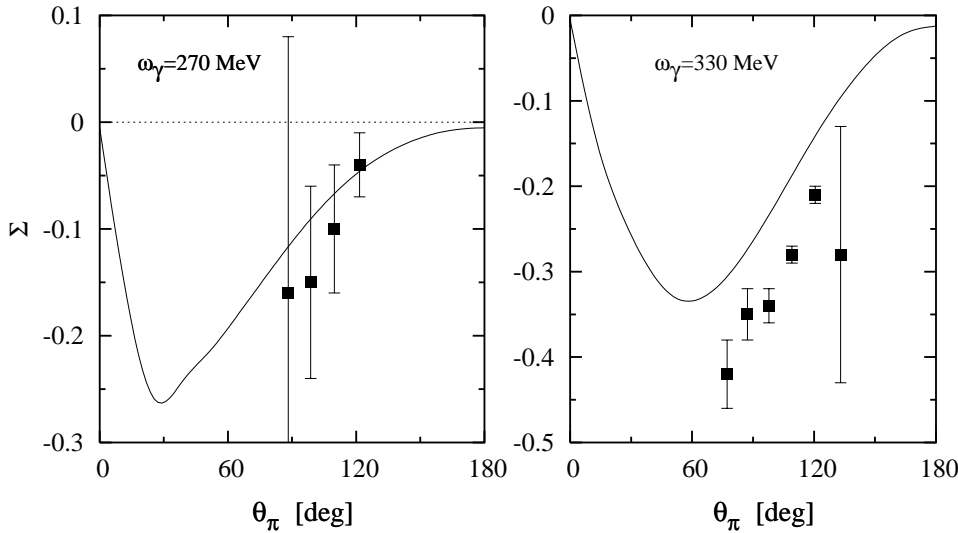


**Figure 2.** Photon beam asymmetry  $\Sigma$  for  $d(\vec{\gamma}, \pi^-)pp$  reaction in comparison with the 'preliminary' experimental data from LEGS [10].

Fig. 2 shows a comparison of our results for the linear photon asymmetry  $\Sigma$  with experimental data. In view of the fact that data for  $\pi^+$  and  $\pi^0$  production channels are not available, we concentrate the discussion on  $\pi^-$  production, for which we have taken the 'preliminary' experimental data from the LEGS Spin collaboration [10]. In agreement with these preliminary data, one can see that the predictions in the pure IA can hardly provide a reasonable description of the data. Major discrepancies are evident which very likely come from the neglect of FSI effects. This means that the simple spectator approach cannot describe the experimental data. Therefore, a careful investigation of FSI effects is necessary. An experimental check of these predictions at wide range of pion angles is needed. Furthermore, an independent evaluation in the framework of effective field theory would be very interesting.

We would like to mention, that we have obtained essentially the same results for the  $\Sigma$ -asymmetry if we take the deuteron wave function of the Bonn r-space potential [17] instead of the deuteron wave function of the Paris one [15].

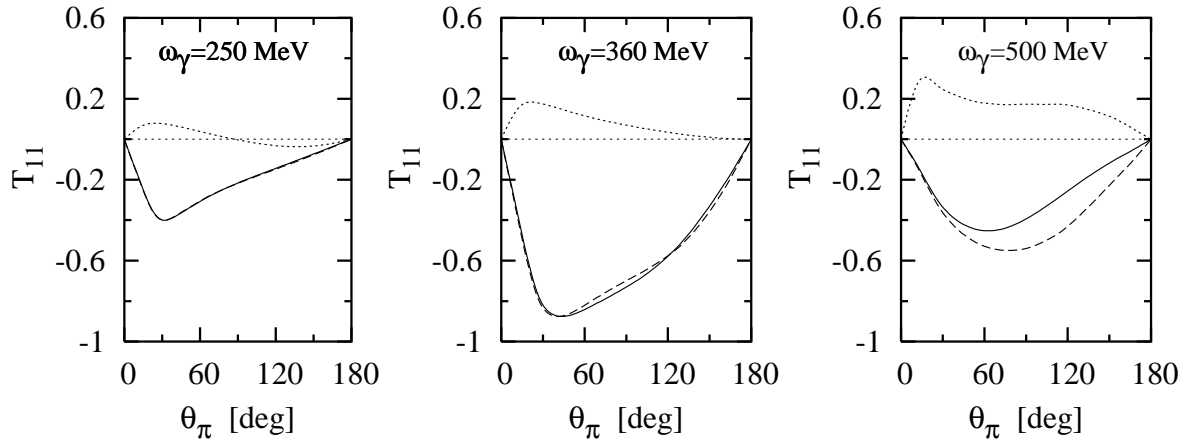


**Figure 3.** Vector target asymmetry  $T_{11}$  of  $\vec{d}(\gamma, \pi)NN$ . Notation as in Fig. 1.

In Fig. 3 we display the results for the vector target asymmetry  $T_{11}$  as a function of pion angle  $\theta_\pi$  at the same values of photon lab-energies as the abovementioned case. It is very clear that the asymmetry  $T_{11}$  has different size in both charged and neutral pion production channels, being even opposite in phase.

For charged pion production channels we see that  $T_{11}$  has negative values, whereas positive values are observed in the case of neutral pion production channel. Only at extreme backward pion angles, very small negative values for  $T_{11}$  is shown in the case of  $\pi^0$ -production channel at  $\omega_\gamma = 250$ . This is because  $T_{11}$  depends on the relative phase of the matrix elements which can be seen from (10) and (16). It would vanish for a constant overall phase of the  $\mathcal{M}$ -matrix. We see also that the  $T_{11}$ -asymmetry is vanished at  $\theta_\pi = 0^\circ$  and  $180^\circ$ . The asymmetry  $T_{11}$  is insensitive to the deuteron wave function, in agreement with the case of photon asymmetry.

In Figs. 4, 5, and 6 we present the results for the tensor target asymmetries  $T_{20}$ ,  $T_{21}$ , and  $T_{22}$ , respectively. Predictions for the three isospin channels of  $\vec{d}(\gamma, \pi)NN$  at three different values of photon lab-energies are given. First we discuss the results for the asymmetry  $T_{20}$  as shown in Fig. 4. For the reaction  $\gamma\vec{d} \rightarrow \pi NN$  at forward and backward emission pion angles, the asymmetry  $T_{20}$  allows one to draw specific conclusions about details of the reaction mechanism.

Comparing with the results for linear photon and vector target asymmetries we found that for charged pion production channels the asymmetry  $T_{20}$  has relatively large positive values at pion forward angles (at  $\theta_\pi < 30^\circ$ ) while small negative ones are found when  $\theta_\pi$  changes from  $30^\circ$  to  $180^\circ$ . For neutral pion production channel, we see that  $T_{20}$  has negative values at forward angles and positive ones at backward angles. Only at energies above the  $\Delta$ -region we observe small negative values at extreme backward angles.

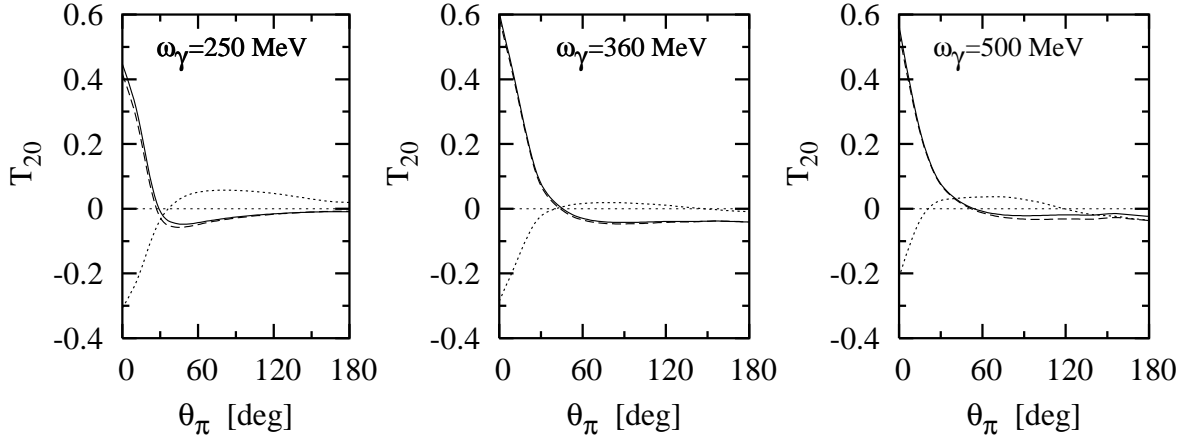


**Figure 4.** Tensor target asymmetry  $T_{20}$  of  $\vec{d}(\gamma, \pi)NN$ . Notation as in Fig. 1.

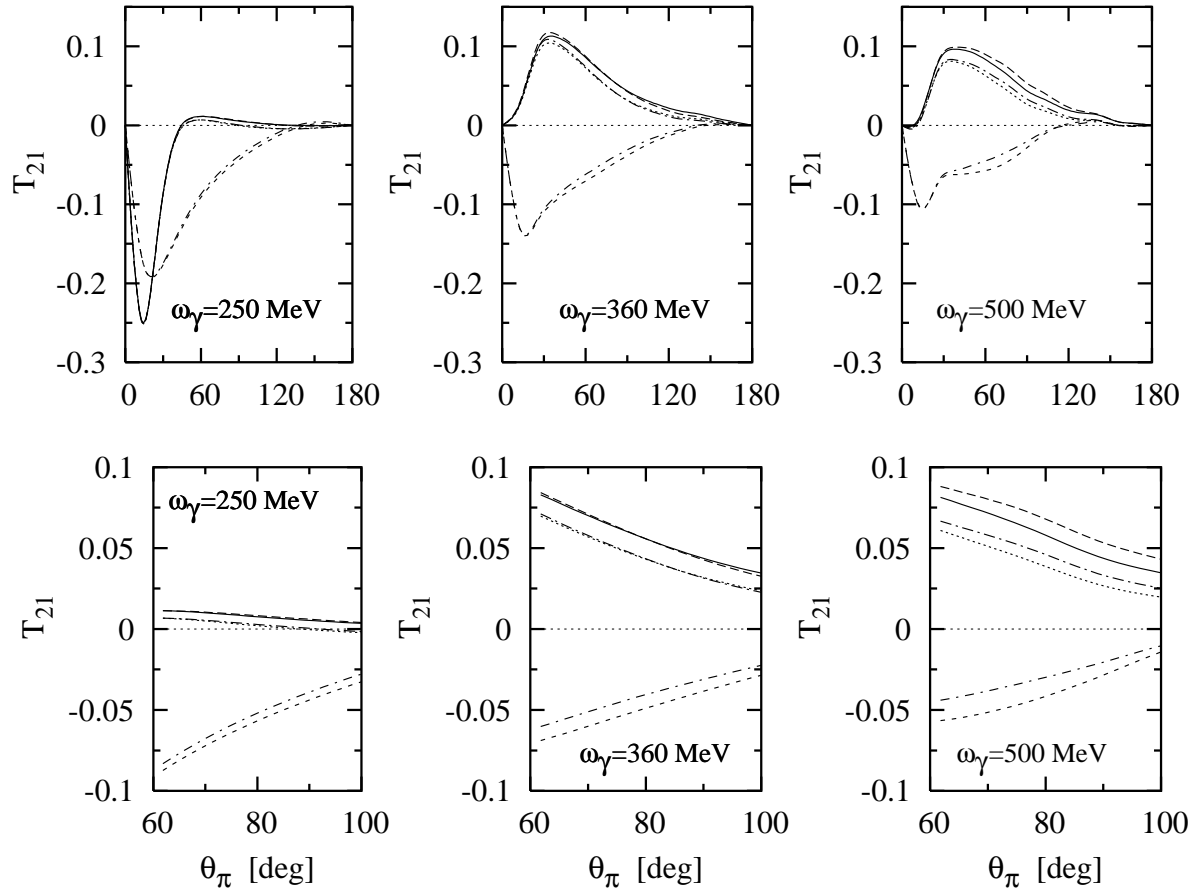


**Figure 5.** Tensor target asymmetry  $T_{21}$  of  $\vec{d}(\gamma, \pi)NN$  at three different values of photon lab-energies. The solid (dotted), long-dashed (long-dashed-dotted), and dashed (dashed-dotted) curves correspond to  $\gamma\vec{d} \rightarrow \pi^- pp$ ,  $\pi^+ nn$ , and  $\pi^0 np$ , respectively, using the deuteron wave function of the Paris [15] (Bonn [17]) potential model. Bottom panels are drawn using enlarged scales from the top ones.

Fig. 5 displays the results for the tensor target asymmetry  $T_{21}$  as a function of pion angle  $\theta_\pi$  using the deuteron wave functions of the Paris and Bonn r-space potential models. It is clear from the top panels that  $T_{21}$  differs in size between charged and neutral pion production channels. In the case of charged pion channels,  $T_{21}$  has relatively large positive values at pion forward angles, which vanished at  $\theta_\pi = 180^\circ$ . Only at low energies we see that  $T_{21}$  is negative at extreme forward angles. For neutral pion channel, it is noticeable that  $T_{21}$  has negative values at forward and backward pion angles. Furthermore, similar to the case in the vector target asymmetry  $T_{11}$ , we found that  $T_{21}$  is vanished at  $\theta_\pi = 0^\circ$  and  $\theta_\pi = 180^\circ$ .

As already observed in the top panels of Fig. 5, we have obtained a noticeable difference in the results of the asymmetry  $T_{21}$  if we take the deuteron wave function of the Bonn potential [17] instead of the wave function of the Paris one [15]. This difference is clear when  $\theta_\pi$  changes from  $60^\circ$  to  $100^\circ$ , in particular for neutral pion channel. At extreme forward and backward emission pion angles, we see that this difference disappears. In order to show this difference in more detail, we display in the bottom panels of Fig. 5 the asymmetry  $T_{21}$  using enlarged scales from the top panels.

In Fig. 6 we depict the results for the tensor target asymmetry  $T_{22}$ . The same values of photon lab-energies as in the previous figures have been used. Similar to the results of Figs. 4 and 5, the  $T_{22}$  asymmetry is sensitive to the values of pion angle  $\theta_\pi$ . We see that, the asymmetry  $T_{22}$  has large positive values for charged pion channels at extreme forward angles which is not the case for neutral pion channels. Moreover, we found that  $T_{22}$  is vanished at  $\theta_\pi = 0^\circ$  and  $180^\circ$ .

Finally, we would like to remark that we have obtained here also different results for the asymmetry  $T_{22}$  if we take the deuteron wave function of the Bonn potential instead of that for the Paris one (see top panels of Fig. 6). The bottom panels of Fig. 6 show this difference in more detail, especially for  $\pi^0$ -production channel at energies above the  $\Delta$ -region. These bottom panels are drawn using enlarged scales from the top ones.

#### 4.2. Beam-target double polarization asymmetries

As already mentioned in the introduction, the main goal of this paper is to present and discuss theoretical results for the double-polarization asymmetries for the reaction  $\vec{d}(\vec{\gamma}, \pi)NN$ . The explicit expressions for these spin observables are given in Appendix A. Interest in double-polarization observables comes from the recent technical improvements of electron accelerator facilities (such as LEGS [10]) with both polarized beams and targets. In view of these recent developments, it will soon be possible to measure double-spin observables with precision.

First of all we would like to emphasize, that using the symmetry relations of the Clebsch-Gordan coefficients  $C_{m_1 m_2 m}^{j_1 j_2 j}$ , the asymmetries  $T_{10}^c$ ,  $T_{11}^c$ ,  $T_{10}^\ell$ , and  $T_{1\pm 1}^\ell$  (see (A.1), (A.3), (A.7), and (A.8), respectively) vanish. One should also note, that obviously for  $\Im m |\mathcal{M}|^2 = 0$ , the asymmetry  $T_{20}^c$  (see (A.4)) vanishes. We found also that the asymmetries  $T_{21}^c$ ,  $T_{22}^c$  and  $T_{2\pm 2}^\ell$  do vanish, whereas the spin asymmetries  $T_{20}^\ell$  and  $T_{2\pm 2}^\ell$

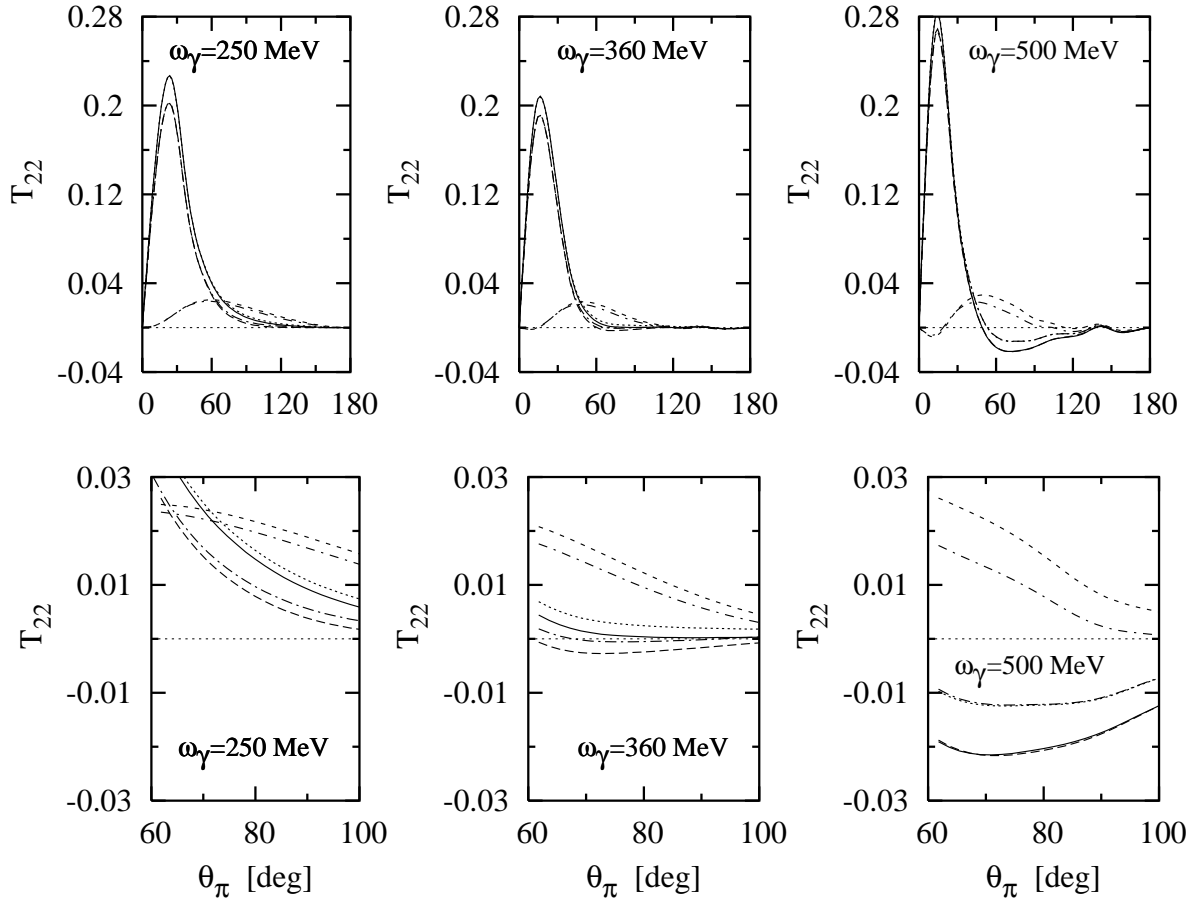


**Figure 6.** Tensor target asymmetry  $T_{22}$  of  $\vec{d}(\gamma, \pi)NN$ . Notation as in Fig. 5.

do not. Moreover, we would like to mention that the values for the  $T_{2+2}^\ell$  asymmetry are found to be identical with the values of  $T_{2-2}^\ell$ . Therefore, in what follows we shall discuss the results for only the  $T_{20}^\ell$  and  $T_{2+2}^\ell$  asymmetries.

Fig. 7 shows the results for the longitudinal double-spin asymmetry  $T_{20}^\ell$  (see (A.9) for its definition) as a function of emission pion angle  $\theta_\pi$  at nine different values of photon lab-energies for the reaction  $\vec{\gamma}\vec{d} \rightarrow \pi NN$ . For  $\pi^0$ -production (dotted curves), we see that  $T_{20}^\ell$  has always positive values at all photon energies and pion angles. Furthermore, it is apparent that at extreme forward and backward emission pion angles the asymmetry  $T_{20}^\ell$  is small in comparison with other angles.

In the case of charged pion production channels ( $\pi^+$ : dashed and  $\pi^-$ : solid curves), we see that  $T_{20}^\ell$  has negative values at forward pion angles around  $\theta_\pi = 30^\circ$  which is not the case at backward angles. These negative values increase (in absolute value decrease) with increasing the photon lab-energy. At extreme backward angles, we see that  $T_{20}^\ell$  has small positive values. The difference between the results for neutral and charged pion channels comes from the fact that the asymmetry  $T_{20}^\ell$  is sensitive to the Born terms, especially at energies above the  $\Delta$ -region.

The results for the longitudinal double-polarization asymmetry  $T_{2+2}^\ell$  (see (A.11)

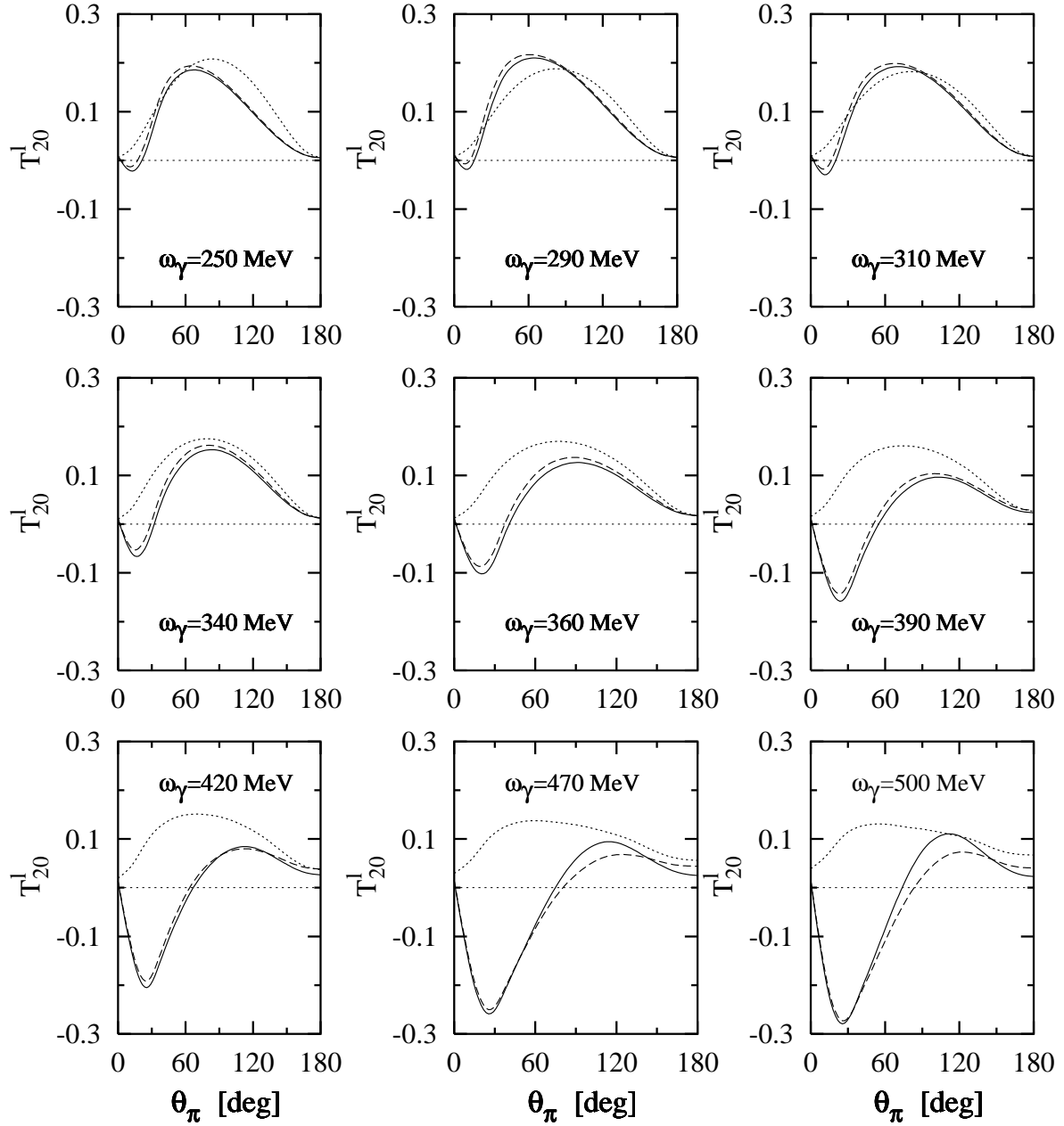


**Figure 7.** The double-polarization asymmetry  $T_{20}^\ell$  of  $\vec{d}(\vec{\gamma}, \pi)NN$  at nine different photon lab-energies. Notation as in Fig. 1.

for its definition) are plotted in Fig. 8 as a function of emission pion angle for all the three charge states of the pion for the reaction  $\vec{\gamma}\vec{d} \rightarrow \pi NN$  at the same nine values of photon lab-energies as the abovementioned case. The solid, dashed, and dotted curves correspond to  $\vec{\gamma}\vec{d} \rightarrow \pi^- pp$ ,  $\pi^+ nn$ , and  $\pi^0 np$ , respectively.

In general, one readily notes that the longitudinal asymmetry  $T_{2+2}^\ell$  has negative values. For neutral and charged pion production channels, it is apparent that the asymmetry  $T_{2+2}^\ell$  has qualitatively the same behaviour. We see also that the values of  $T_{2+2}^\ell$  for  $\pi^0$  channel are greater (in absolute value smaller) than its values for  $\pi^\pm$

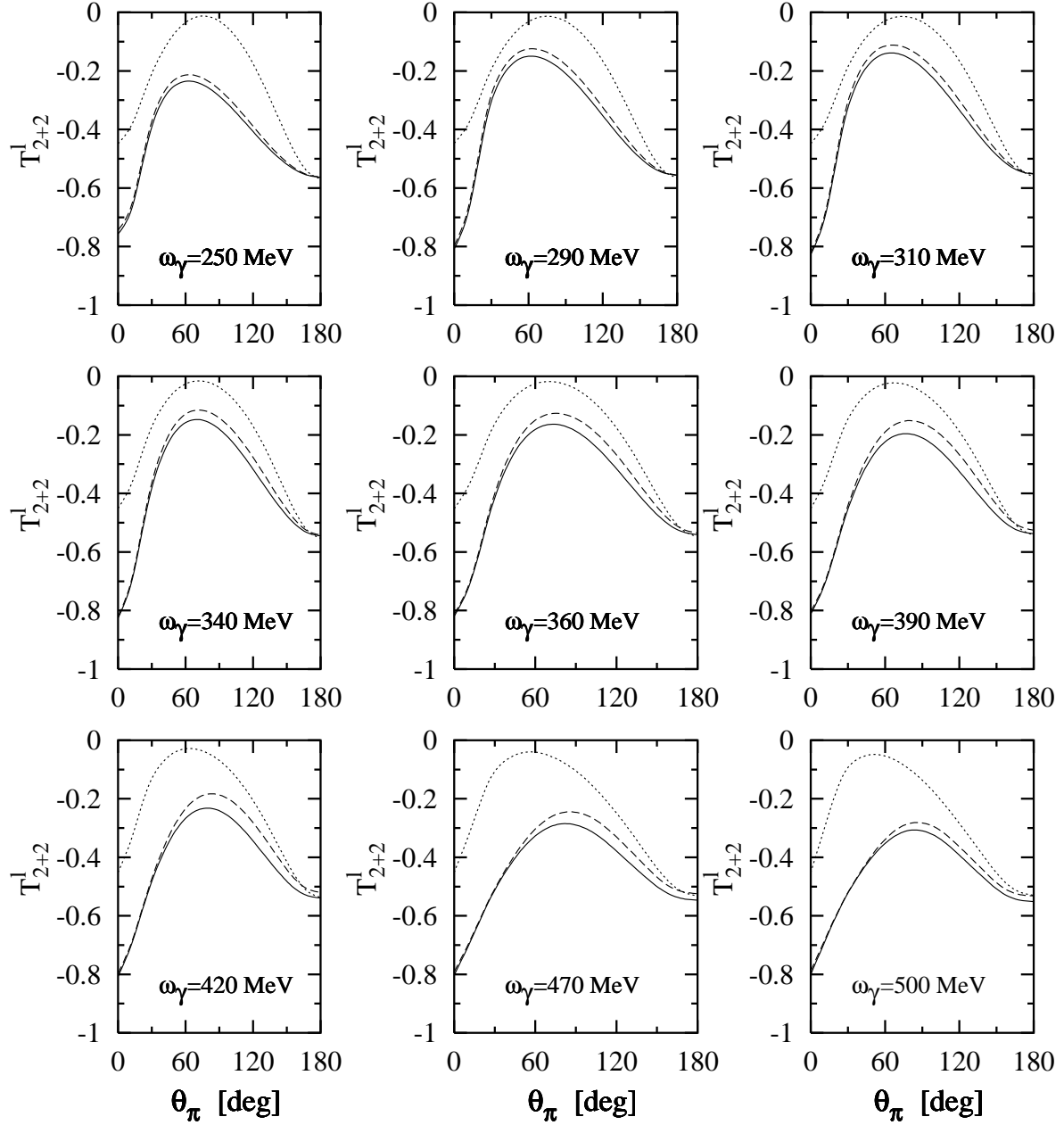


**Figure 8.** The double-polarization asymmetry  $T_{2+2}^\ell$  of  $\vec{d}(\vec{\gamma}, \pi)NN$  at nine different photon lab-energies. Notation as in Fig. 1.

channels, in particular at  $\theta_\pi = 0^\circ$ . Furthermore, we noticed that the values of  $T_{2+2}^\ell$  in the case of  $\pi^0$ -production are insensitive to the photon energy and/or pion angle, which is not the case for  $\pi^\pm$ -production channels. It is very interesting to examine these asymmetries experimentally.

Last but not least, we would like to mention that the results for double-spin asymmetries are insensitive to the deuteron wave function of a particular potential model as discussed above for the single-spin asymmetries  $T_{21}$  and  $T_{22}$ . This means, that we have obtained essentially the same results for the double-spin asymmetries if we take

the deuteron wave function of the Bonn r-space potential [17] instead of the deuteron wave function of the Paris potential model [15].

## 5. Conclusions and outlook

In this paper we have presented predictions for polarization observables for incoherent single-pion photoproduction on the deuteron in the  $\Delta(1232)$ -resonance region. Special emphasize is given for the beam-target double-spin asymmetries, for which the explicit formal expressions are given. The elementary  $\pi$ -photoproduction operator on the free nucleon is taken in an effective Lagrangian model which describes well the elementary reaction. For the deuteron wave function, the realistic Paris potential model is used.

It has been found, that the beam spin asymmetry  $\Sigma$  and the target spin asymmetries  $T_{11}$ ,  $T_{20}$ ,  $T_{21}$ , and  $T_{22}$  do not vanish. For the beam-target double-spin asymmetries, it is found that only the asymmetries  $T_{20}^\ell$  and  $T_{2\pm 2}^\ell$  for longitudinal photon and deuteron target do not vanish, whereas all the asymmetries for circular photon and deuteron target and the other asymmetries for longitudinal photon and deuteron target do vanish. In comparison with experimental data for the linear photon asymmetry, big differences between our predictions and the 'preliminary' data from LEGS [10] are found which very likely come from the neglect of FSI effects in our model.

The sensitivity of our results for single- and double-spin asymmetries to the deuteron wave function has been investigated. For this purpose the deuteron wave function of the Bonn potential has been used. We found that only the tensor target asymmetries  $T_{21}$  and  $T_{22}$  are sensitive to the deuteron wave function of a particular  $NN$  potential model, in particular in the case of neutral pion photoproduction channel at photon energies above the  $\Delta(1232)$ -resonance region, and that all other single- and double-spin asymmetries are not. An experimental check of these predictions for polarization observables would provide an additional significant test of our present understanding of low-energy behaviour of few-body nuclei. Furthermore, in view of this low-energy property, an independent calculations in the framework of effective field theory would be very interesting.

In summary, we would like to point out that future improvements of the present approach should include a more sophisticated elementary production operator, which will allow one to extend the present approach to higher energies, and the role of final-state interactions as well as two-body effects to the electromagnetic pion production operator. This approach is necessary for the problem at hand since the polarization observables are sensitive to the dynamical effects. Moreover, the formalism can also be extended to investigate polarization observables of pion electroproduction on the deuteron where the virtual photon has more degrees of freedom than the real one. Therefore, it can be used to explore the reaction more deeply.

## Appendix A. Explicit expressions for double-spin asymmetries

In this appendix the explicit formal expressions for the various double-polarization asymmetries listed in (18) through (21) in terms of the transition  $\mathcal{M}$ -matrix elements are given.

(A) Asymmetries for circular photon and deuteron target

$$\begin{aligned} T_{10}^c &= \frac{\sqrt{3}}{\mathcal{F}} \operatorname{Re} \sum_{smtm_\gamma m_d m'_d} \int_0^{q_{\max}} dq \int d\Omega_{p_{NN}} \rho_s (-)^{1-m'_d} C_{m_d-m'_d 0}^{111} \\ &\quad \times \mathcal{M}_{smm_\gamma m_d}^{(t\mu)} \star \mathcal{M}_{smm_\gamma m'_d}^{(t\mu)} \\ &= 0, \end{aligned} \quad (\text{A.1})$$

where  $\mathcal{F}$  is given by

$$\mathcal{F} = \sum_{smtm_\gamma m_d} \int_0^{q_{\max}} dq \int d\Omega_{p_{NN}} \rho_s |\mathcal{M}_{smm_\gamma m_d}^{(t\mu)}|^2, \quad (\text{A.2})$$

$$\begin{aligned} T_{11}^c &= \frac{-2\sqrt{3}}{\mathcal{F}} \operatorname{Re} \sum_{smtm_\gamma m_d m'_d} \int_0^{q_{\max}} dq \int d\Omega_{p_{NN}} \rho_s (-)^{1-m'_d} C_{m_d-m'_d 1}^{111} \\ &\quad \times \mathcal{M}_{smm_\gamma m_d}^{(t\mu)} \star \mathcal{M}_{smm_\gamma m'_d}^{(t\mu)} \\ &= 0, \end{aligned} \quad (\text{A.3})$$

$$\begin{aligned} T_{20}^c &= \frac{\sqrt{2}}{\mathcal{F}} \Im m \sum_{smtm_\gamma} \int_0^{q_{\max}} dq \int d\Omega_{p_{NN}} \rho_s \left[ |\mathcal{M}_{smm_\gamma+1}^{(t\mu)}|^2 + |\mathcal{M}_{smm_\gamma-1}^{(t\mu)}|^2 \right. \\ &\quad \left. - 2 |\mathcal{M}_{smm_\gamma 0}^{(t\mu)}|^2 \right] \\ &= 0, \end{aligned} \quad (\text{A.4})$$

$$\begin{aligned} T_{21}^c &= \frac{-\sqrt{6}}{\mathcal{F}} \Im m \sum_{smtm_\gamma} \int_0^{q_{\max}} dq \int d\Omega_{p_{NN}} \rho_s \left[ \mathcal{M}_{smm_\gamma 0}^{(t\mu)} \star \mathcal{M}_{smm_\gamma-1}^{(t\mu)} \right. \\ &\quad \left. - \mathcal{M}_{smm_\gamma+1}^{(t\mu)} \star \mathcal{M}_{smm_\gamma 0}^{(t\mu)} \right], \end{aligned} \quad (\text{A.5})$$

$$T_{22}^c = \frac{2\sqrt{3}}{\mathcal{F}} \Im m \sum_{smtm_\gamma} \int_0^{q_{\max}} dq \int d\Omega_{p_{NN}} \rho_s \mathcal{M}_{smm_\gamma+1}^{(t\mu)} \star \mathcal{M}_{smm_\gamma-1}^{(t\mu)}. \quad (\text{A.6})$$

(B) Asymmetries for longitudinal photon and deuteron target

$$\begin{aligned} T_{10}^\ell &= \frac{i\sqrt{3}}{\mathcal{F}} \sum_{smtm_\gamma m_d m'_d} \int_0^{q_{\max}} dq \int d\Omega_{p_{NN}} \rho_s (-)^{1-m'_d} C_{m_d-m'_d 0}^{111} \\ &\quad \times \mathcal{M}_{smm_\gamma m_d}^{(t\mu)} \star \mathcal{M}_{s-mm_\gamma-m'_d}^{(t\mu)} \\ &= 0, \end{aligned} \quad (\text{A.7})$$

$$\begin{aligned} T_{1\pm 1}^\ell &= \frac{-i\sqrt{3}}{\mathcal{F}} \sum_{smtm_\gamma m_d m'_d} \int_0^{q_{\max}} dq \int d\Omega_{p_{NN}} \rho_s (-)^{1-m'_d} C_{m_d-m'_d \pm 1}^{111} \\ &\quad \times \mathcal{M}_{smm_\gamma m_d}^{(t\mu)} \star \mathcal{M}_{s-mm_\gamma-m'_d}^{(t\mu)} \\ &= 0, \end{aligned} \quad (\text{A.8})$$

$$T_{20}^\ell = \frac{-1}{\sqrt{2}\mathcal{F}} \sum_{smtm_\gamma} \int_0^{q_{\max}} dq \int d\Omega_{p_{NN}} \rho_s \left[ \mathcal{M}_{smm_\gamma-1}^{(t\mu)} \star \mathcal{M}_{s-mm_\gamma+1}^{(t\mu)} \right. \\ \left. + \mathcal{M}_{smm_\gamma+1}^{(t\mu)} \star \mathcal{M}_{s-mm_\gamma-1}^{(t\mu)} - 2 \mathcal{M}_{smm_\gamma 0}^{(t\mu)} \star \mathcal{M}_{s-mm_\gamma 0}^{(t\mu)} \right], \quad (\text{A.9})$$

$$T_{2\pm 1}^\ell = \frac{\sqrt{3}}{\sqrt{2}\mathcal{F}} \sum_{smtm_\gamma} \int_0^{q_{\max}} dq \int d\Omega_{p_{NN}} \rho_s \left[ \pm \mathcal{M}_{smm_\gamma 0}^{(t\mu)} \star \mathcal{M}_{s-mm_\gamma \pm 1}^{(t\mu)} \right. \\ \left. \mp \mathcal{M}_{smm_\gamma \pm 1}^{(t\mu)} \star \mathcal{M}_{s-mm_\gamma 0}^{(t\mu)} \right], \quad (\text{A.10})$$

$$T_{2\pm 2}^\ell = \frac{-\sqrt{3}}{\mathcal{F}} \sum_{smtm_\gamma} \int_0^{q_{\max}} dq \int d\Omega_{p_{NN}} \rho_s \mathcal{M}_{smm_\gamma \pm 1}^{(t\mu)} \star \mathcal{M}_{s-mm_\gamma \pm 1}^{(t\mu)}. \quad (\text{A.11})$$

## Acknowledgements

I am gratefully acknowledge very useful discussions with Prof. H. Arenhövel as well as the members of his work group. I am also indebted to Prof. T.-S. Harry Lee for fruitful discussions. I would like to thank Dr. M. Abdel-Aty for a careful reading of the manuscript.

## References

- [1] Laget, J. M.: Phys. Rep. **69**, 1 (1981).
- [2] Krusche, B. and Schadmand, S.: Prog. Part. Nucl. Phys. **51**, 399 (2003).
- [3] Burkert, V. and Lee, T.-S. H.: Int. J. Mod. Phys. **E**, (2004), nucl-th/0407020.
- [4] Drechsel, D. and Tiator, L.: nucl-th/0406059.
- [5] Loginov, A. Yu., Sidorov, A. A. and Stibunov, V. N.: Phys. Atom. Nucl. **63**, 391 (2000).
- [6] Darwish, E. M., Arenhövel, H. and Schwamb, M.: Eur. Phys. J. **A16**, 111 (2003).
- [7] Darwish, E. M., Arenhövel, H. and Schwamb, M.: Eur. Phys. J. **A17**, 513 (2003).
- [8] Darwish, E. M.: Nucl. Phys. **A735**, 200 (2004).
- [9] Darwish, E. M.: Int. J. Mod. Phys. **E13**, (2004) (in print).
- [10] Lucas, M.: in *LOWq 2001 Workshop on Electromagnetic Nuclear Reactions at Low Momentum Transfer*, Halifax, Nova Scotia, Canada, 23-25 August, 2001 and private communication.
- [11] Sandorfi, A.: in *Proceedings of the 2nd Int. Symposium on the Gerasimov-Drell-Hearn 2002 Sum Rule and the Spin Structure of the Nucleon*, Genova, Italy, 3-6 July, 2002, edited by Anghinolfi, M., Battaglieri, M. and De Vita, R. (World Scientific, Singapore, 2003) and private communication.
- [12] Bjorken, J. D. and Drell, S. D.: *Relativistic Quantum Mechanics* (McGraw-Hill, New York, 1964).
- [13] Arenhövel, H.: Few-Body Syst. **4**, 55 (1988).
- [14] Edmonds, A. R.: *Angular Momentum in Quantum Mechanics* (Princeton University Press, New Jersey, 1957).
- [15] Lacombe, M. et al.: Phys. Lett. **B101**, 139 (1981).
- [16] Schmidt, R., Arenhövel, H. and Wilhelm, P.: Z. Phys. **A355**, 421 (1996).
- [17] Machleidt, R., Holinde, K. and Elster, Ch.: Phys. Rep. **149**, 1 (1987); Machleidt, R.: Adv. Nucl. Phys. **19**, 189 (1989).